Progress In Electromagnetics Research, PIER 21, 307–318, 1999

THE APPLICATION OF MOM AND EECS ON EM SCATTERING FROM SLOT ANTENNAS

M. Zhang

Shaanxi Astronomical Observatory
Academia Sinica
Lintong, 710600,
P.R. China

Z. Wu

Department of Physics
Xidian University of Electronic Science and Technology
Xi'an 710071, Shaanxi
P.R. China

1. INTRODUCTION

Waveguide-fed slot antennas are widely used on airborne radars. Based on the characteristics of the antennas, they are described as a structure

of rectangular waveguides in the same size and longitudinal slots flush-mounted on them. Although these antennas have been studied for many years, they were treated mainly as radiating structures, with the major concern on radiation patterns. However, research on the EM scattering characteristics of these antennas is of significance in targets (especially on complex targets) identification.

In this paper, a numerical technique employing the MOM and EECs is presented for studying the scattering from slot antennas fed by waveguides with arbitrary terminations. The fields in the slot's are calculated by assuming slots array which are mounted flush on a large conducting plane, and the total fields are evaluated approximately by overlapping the slots fields with the fields of the conducting plane. However, the methods described in many previous literatures mainly deal with the slots, not the conducting plane. Chen and Jin [1] employed the MOM to solve the field in the waveguide-fed slot. Recently, Fan and Jin [3] analyzed the scattering from a conformal slotted waveguide array antenna. In practice, we find that the method following described is more applicable.

2. FORMULATIONS

The geometry of waveguide-fed slots in a conducting plane is shown in Fig. 1.

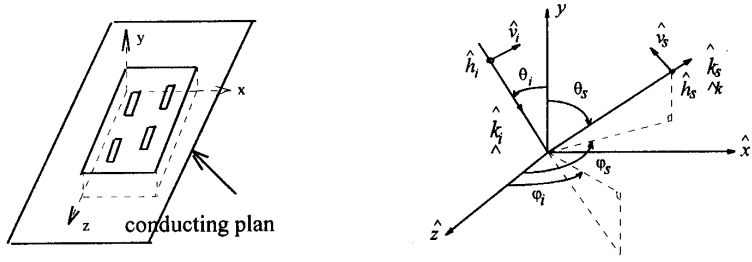

Figure 1. Geometry of waveguide-fed slots in a conducting plane and its coordinate system.

2.1 Scattering of Waveguide-Fed Slots

It is assumed that the slot arrays are flush-mounted on an infinite conducting plane. In accordance with the field equivalence principle,

the equivalent magnetic currents above and below the slot of a perfectly conducting surface are introduced. Because of the continuity of the tangential electric fields across the apertures, the directions of the equivalent magnetic currents above and below the aperture are opposite. According to the MOM, for the ith slot, its equivalent magnetic current is:

$$\vec{M}_i = \hat{n} \times \vec{E}_s \tag{1}$$

where $\vec{E}_s$ is the fields scattered by the slots.

The integral equation satisfied by the equivalent magnetic currents is obtained as

$$\sum_j \vec{H}_{ti}^{in}\left(\vec{M}_j\right) + \sum_j \vec{H}_{ti}^{ex}\left(\vec{M}_j\right) = \vec{H}_{ti}^{pri} \tag{2}$$

where the subscript t denotes the tangential component. $\vec{H}^{pri}$ is the fields due to the incidence in the presence of the conducting plane without slots. $\vec{H}^{in}$, $\vec{H}^{ex}$ refer to the magnetic field by the internal and external surface magnetic current, respectively.

$$\vec{H}^{ex}(\vec{r}) = -j\omega\varepsilon_0 \iint_s \overline{\overline{G}}^{ex}\left(\vec{r}, \vec{r}\,'\right) \cdot \vec{M}\left(\vec{r}\,'\right) ds' \tag{3a}$$

$$\vec{H}^{in}(\vec{r}) = -j\omega\varepsilon_0 \iint_s \overline{\overline{G}}^{in}\left(\vec{r}, \vec{r}\,'\right) \cdot \vec{M}\left(\vec{r}\,'\right) ds' \tag{3b}$$

where $\overline{\overline{G}}^{ex}\left(\vec{r}, \vec{r}\,'\right)$, and $\overline{\overline{G}}^{in}\left(\vec{r}, \vec{r}\,'\right)$ denote the dyadic Green's functions of the outer and inner surfaces.

In general, the slots are so narrow for C, X, Ka. Ku bands that it can be assumed that there is only transverse electric fields component across the slots, and the magnetic current is only along the longitudinal direction. Each equivalent magnetic current is expended by using the global sinusoidal basis functions [1]

$$\vec{M}_j = \hat{z} M_j = \hat{z} \sum_q^N V_{qj} B_{qj}(z) \tag{4}$$

$$B_{qj}(z) = \sin\left[\frac{q\pi}{L}\left(L + z - z_j\right)\right] \tag{5}$$

where L is the length of the slot, z_j is the center position of the jth slot. By applying Galerkin's procedure, the integral equations can be converted into the matrix given by

$$\left[Y_{pq}^{ij}\right] \times [V_{qj}] = [I_{pi}] \tag{6}$$

where

$$Y_{pq}^{ij} = \begin{cases} Y_{pq}^{ij}(ex) + Y_{pq}^{ij}(in) & \text{slots on a waveguide} \\ Y_{pq}^{ij}(ex) & \text{slots on different waveguide} \end{cases}$$

$Y_{pq}^{ij}(ex)$ and $Y_{pq}^{ij}(in)$ are the generalized admittance matrix for external and internal of waveguides, respectively.

2.1.1 Generalized Admittance Matrix Elements for the Internal of Waveguide

It is known that

$$Y_{pq}^{ij}(in) = -j\omega\varepsilon_0 \iint_{S_i} \iint_{S_j} G_{zz}^{in}\left(\vec{r}, \vec{r}\,'\right) \sin B_{pi}(z) \sin B_{qj}(z')\, dsds' \tag{7}$$

where G_{zz}^{in} is the zz component of the dyadic Green's function for the waveguide

$$G_{zz}^{in}\left(\vec{r}, \vec{r}\,'\right) = \left(k^2 + \frac{\partial^2}{\partial z^2}\right) g_{zz}\left(\vec{r}, \vec{r}\,'\right) \tag{8}$$

$$\begin{aligned} g_{zz}\left(\vec{r}, \vec{r}\,'\right) = & \sum_{m=0}^{\infty} \sum_{n=0}^{\infty} \frac{j\varepsilon_m \varepsilon_n}{2abk_{mn}} e^{jk_{mn}|z-z'|} \\ & \cdot \cos\frac{m\pi x}{a} \cos\frac{m\pi x'}{a} \cos\frac{n\pi y}{b} \cos\frac{n\pi y'}{b} \end{aligned} \tag{9}$$

where $\varepsilon_m = \begin{cases} 1, & m = 0 \\ 2, & m \neq 0 \end{cases}$, $k_m = \sqrt{k^2 - \left(\frac{m\pi}{a}\right)^2 - \left(\frac{n\pi}{b}\right)^2}$, k is the free space wave number for a waveguide with a cross section $a \times b$. Substituting (8) and (9) into (7),
when $z_i > z_j$,

$$\begin{aligned} Y_{pq}^{ij}(in) = & \sum_{m=0}^{\infty} \sum_{n=0}^{\infty} B_{mn}^{ij} \frac{k_p k_q \left(k^2 - k_{mn}^2\right) \exp(jk_{mn}(z_i - z_j))}{\left(k_p^2 - k_{mn}^2\right)\left(k_q^2 - k_{mn}^2\right) k_{mn}} \\ & \cdot \left[1 - (-1)^p e^{jk_{mn}L}\right] \left[1 - (-1)^q e^{-jk_{mn}L}\right] \end{aligned} \tag{10}$$

when $z_i < z_j$

$$Y_{pq}^{ij}(in) = \sum_{m=0}^{\infty}\sum_{n=0}^{\infty} B_{mn}^{ij} \frac{k_p k_q \left(k^2 - k_{mn}^2\right) \exp(jk_{mn}(z_j - z_i))}{\left(k_p^2 - k_{mn}^2\right)\left(k_q^2 - k_{mn}^2\right) k_m n} \cdot \left[1 - (-1)^p e^{-jk_{mn}L}\right]\left[1 - (-1)^q e^{jk_{mn}L}\right] \tag{11}$$

when $z_i = z_j$

$$Y_{pq}^{ij}(in) = \sum_{m=0}^{\infty}\sum_{n=0}^{\infty} B_{mn}^{ii} \frac{-jL\left(k^2 - k_p k_q\right)}{\left(k_q^2 - k_{mn}^2\right)}\delta_{pq} + \sum_{m=0}^{\infty}\sum_{n=0}^{\infty} B_{mn}^{ii} \frac{2k_p k_q \left(k^2 - k_{mn}^2\right)}{\left(k_p^2 - k_{mn}^2\right)\left(k_q^2 - k_{mn}^2\right) k_{mn}} \cdot \begin{cases} 1 - e^{jk_{mn}L}, & \text{both } p,\ q \text{ are even number} \\ 1 + e^{jk_{mn}L}, & \text{both } p,\ q \text{ are odd number} \end{cases} \tag{12}$$

where $k_p = \frac{p\pi}{L}$, $k_q = \frac{q\pi}{L}$, $\delta_{pq} = \begin{cases} 1, & p = q \\ 0, & p \neq q \end{cases}$, $B_{mn}^{ij} = \frac{j\varepsilon_m \varepsilon_n w^2}{2ab} \sin c^2 \cdot \left(\frac{m\pi w}{2a}\right) \cos\left(\frac{m\pi x_i}{a}\right) \cos\left(\frac{m\pi x_j}{a}\right)$, and w is the width of the slot.

2.1.2 Generalized Admittance Matrix Elements for the External of Waveguide

$$Y_{pq}^{ij}(ex) = -j\omega\varepsilon_0 \iint_{S_i}\iint_{S_j} G_{zz}^{ex}\left(\vec{r}, \vec{r}\,'\right) \sin B_{pi}(z) \cdot \sin B_{qj}(z') ds ds' \tag{13}$$

where G_{zz}^{ex} is the zz component of the dyadic Green's function for half free-space.

$$G_{zz}^{ex}\left(\vec{r}, \vec{r}\,'\right) = \left(k^2 + \frac{\partial^2}{\partial z^2}\right) \frac{e^{-jkR}}{2\pi R} \tag{14}$$

where $R = \sqrt{(x - x')^2 + (y - y')^2}$ is the distance between the integration point at the aperture and the observation point. We also can obtain

$$Y_{pq}^{ij}(ex) = k^2 \iint_{S_i}\iint_{S_j} \frac{\exp(-jkR)}{2\pi R} \sin k_p \left(\frac{L}{2} + z - z_i\right)$$

$$\cdot \sin k_q \left(\frac{L}{2} + z' - z_j\right) dSdS'$$
$$- k_p k_q \iint_{S_i} \iint_{S_j} \frac{\exp(-jkR)}{2\pi R} \cos k_p \left(\frac{L}{2} + z - z_i\right)$$
$$\cdot \cos k_q \left(\frac{L}{2} + z' - z_j\right) dSdS' \tag{15}$$

which can be evaluated by using Gaussian quadrature. However, when $i = j$, the singularity will occur. In order to eliminate it, we can evaluate the integration by transformation of variables

$$Y_{pq}^{ii}(ex) = \frac{1 + (-1)^{p+q}}{2\pi} \left\{ \int_0^{\theta_0} \int_0^{\frac{L}{\cos\theta}} + \int_{\theta_0}^{\frac{\pi}{2}} \int_0^{\frac{w}{\sin\theta}} \right\} e^{-jk\rho} F(\rho, \theta) d\rho d\theta \tag{16}$$

where

$$F(\rho,\theta) = \begin{cases} \dfrac{2(w - \rho\sin\theta)}{k_p^2 - k_q^2} \left[k_p \left(k^2 - k_q^2\right) \sin(k_q \rho \cos\theta)\right. \\ \qquad \left. - k_q \left(k^2 - k_p^2\right) \sin(k_p \rho \cos\theta)\right], & p \neq q \\ (w - \rho\sin\theta)\Big[(L - \rho\cos\theta)\left(k^2 - k_p^2\right)\cos(k_p\rho\cos\theta) \\ \qquad + \dfrac{1}{k_p}\left(k^2 + k_p^2\right)\sin(k_p\rho\cos\theta)\Big], & p = q \end{cases} \tag{17}$$

2.1.3 The Elements of Excitation Vector

With the assumption that the conducting plane is infinite, the elements of excitation vector can be expressed in terms of the incident fields

$$I_{pi} = \frac{2jkZ_0 w k_p H_z^{inc}}{k_p^2 - k_z^2} \sin c\left(\frac{k_{ix} w}{2}\right) \cdot e^{-j(k_{ix}x_i + k_{iz}z_i)} e^{jk_{iz}L/2}$$
$$\cdot \left[1 - (-1)^p e^{-jk_{iz}L}\right] \tag{18}$$

where k_{ix}, k_{iz} are x, z component of $\vec{k}_i$. $\vec{k}_i = k\sin\theta_i(\cos\varphi_i\hat{z} + \sin\varphi_i\hat{x}) - \cos\theta_i\hat{y}$, $k_{ix} = k\sin\theta_i\sin\varphi_i$, $k_{iz} = k\sin\theta_i\cos\varphi_i$, $H_z^{inc} = -H_0(\cos\theta_i\cos\varphi_i + \sin\varphi_i)$.

2.1.4 Far Scattered Fields of Slots Array

By Eq. (3a), the far scattered fields can be expressed as

$$\begin{aligned}\vec{H}^s(\vec{r}) &= -j\omega\varepsilon_0\frac{\exp(-jkr)}{2\pi r}\left(\hat{\theta}_s\hat{\theta}_s+\hat{\varphi}_s\hat{\varphi}_s\right)\cdot\sum_{i=1}^{M}\iint_{S_i}\vec{M}_i e^{j\vec{k}_s\cdot\vec{r}\,'}ds' \\ &= -j\omega\varepsilon_0\frac{\exp(-jkr)}{2\pi r}\left(\hat{\theta}_s\hat{\theta}_s+\hat{\varphi}_s\hat{\varphi}_s\right) \\ &\quad\cdot\hat{z}\sum_{i=1}^{M}\left\{e^{j(k_{sx}x_i+k_{sz}z_i)}e^{-jk_{sz}L/2}w\sin c\left(\frac{k_{sx}w}{2}\right)\right. \\ &\quad\left.\cdot\left[\sum_{p=1}^{N}\frac{V_{pi}k_p\left(1-(-1)^p e^{jk_{sz}L}\right)}{k_p^2-k_{sz}^2}\right]\right\}\end{aligned} \tag{19}$$

where $\vec{k}_s = k\sin\theta_s(\cos\varphi_s\hat{z}+\sin\varphi_s\hat{x})+\cos\theta_s\hat{y}k_{sx} = k\sin\theta_s\sin\varphi_s$, $k_{sz}=k\sin\theta_s\cos\varphi_s$, and $\sin c(x)=\frac{\sin x}{x}$.

2.2 Far-Zone Scattered Fields From Large Conducting Plane

The effect of the conducting plane with finite size on scattering of the antenna should be considered. By using the method of EECs, the scattered fields is [5–6]

$$\vec{E}_S = jk_0\int_C\left[\eta_0 I(\vec{r})\,\hat{k}_S\times\left(\hat{k}_S\times\hat{t}\right)+M(\vec{r})\left(\hat{k}_S\times\hat{t}\right)\right]\cdot\frac{\exp(-jk_0S)}{4\pi S}dl \tag{20}$$

where k_0: the free space wave number, η_0: intrinsic impedance of the medium, $\hat{k}_S$: unit vector in the direction of the observation point, $\hat{t}$: unit vector along the edge, I, M: the equivalent edge currents assumed at the edge of a planar scattering, respectively. $S=|\vec{r}\,'-\vec{r}|$: the distance between a point on the edge and the observation.

For diffraction points on the *Keller* cone, the I, M can be expressed as

$$\begin{aligned}I^{GTD} &= \frac{2jE_t^i}{k_0\eta_0\sin^2\beta}D_e^{GTD}+\frac{2jH_t^i}{k_0\sin\beta}D_{em}^{GTD}, \\ M^{GTD} &= \frac{2j\eta_0 H_t^i}{k_0\sin^2\beta}D_m^{GTD}.\end{aligned} \tag{21}$$

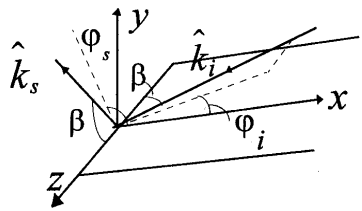

Figure 2. A local coordinate system at the edge point.

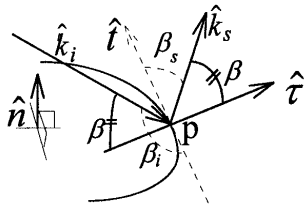

Figure 3. Definition of the fictitious edge $\hat{\tau}$.

$$\begin{aligned} D_e^{GTD} &= \frac{1}{2}\left[\sec\left(\frac{\varphi_s-\varphi_i}{2}\right)-\sec\left(\frac{\varphi_s+\varphi_i}{2}\right)\right], \\ D_m^{GTD} &= -\frac{1}{2}\left[\sec\left(\frac{\varphi_s-\varphi_i}{2}\right)+\sec\left(\frac{\varphi_s+\varphi_i}{2}\right)\right],\ D_{em}^{GTD}=0. \end{aligned} \tag{22}$$

where the coordinate system and symbols are shown in Fig. 2. Furthermore, the modified edge is defined in Fig. 3.

$$\begin{cases} \hat{\tau}=\hat{t} & \text{for points on SB/RB} \\ \left(\hat{k}_s-\hat{k}_i\right)\cdot\hat{t}=0,\ \hat{n}\cdot\hat{\tau}=0 & \text{for general points} \end{cases} \tag{23}$$

For general points

$$\hat{\tau}=\pm\frac{\hat{n}\times\left(\hat{k}_s-\hat{k}_i\right)}{\left|\hat{n}\times\left(\hat{k}_s-\hat{k}_i\right)\right|} \tag{24}$$

Then, the EECs by modified edge representation and the scattering fields are obtained as follow [5–6]:

(a) A local spherical coordinate system with the z-axis along the fictitious edge $\hat{\tau}$ is considered at the edge point P.
(b) I, M are calculated for the fictitious edge $\hat{\tau}$ using Eq. (21).

(c) The diffracted far fields are calculated by Eq. (20). It is noted that the direction of EECs is taken along the original edge $\hat{t}$.

The variables of Eqs. (21) and (22) can be calculated by

$$E_t^i = \vec{E}^i \cdot \hat{\tau}, \quad H_t^i = \vec{H}^i \cdot \hat{\tau}, \quad \beta = \cos^{-1}\left(-\hat{k}_i \cdot \hat{\tau}\right)$$
$$\varphi_i = \tan^{-1}\left(\frac{-\hat{k}_i \cdot \hat{x}'}{-\hat{k}_i \cdot \hat{y}'}\right), \quad \varphi_s = \tan^{-1}\left(\frac{\hat{k}_s \cdot \hat{x}'}{\hat{k}_s \cdot \hat{y}'}\right).$$
$$0 \le \varphi_i \le \pi, \qquad 0 \le \varphi_s \le 2\pi \tag{25}$$

3. NUMERICAL RESULTS

The formulae described above have been implemented in a computer program and a variety of numerical results are obtained to demonstrate the effects of various factors on RCS. In this article we study mainly on the frequency characteristics of scattering from the slot antenna.

The first case calculated is the scattering from a single slot on a 22×7 mm waveguide. The slot is 1.5 mm wide and 15 mm long. The RCS of this structure terminated by a perfect conductor is shown in Fig. 4 over a large frequency range. It can be concluded that:

(a) In frequency bands between 4 and 12 GHz, the computation using Eq. (4) needs only $N = 1$, between 12 and 35 GHz, $N = 3$, between 35 and 40 GHz, $N = 5$. The higher the frequency, the larger the number N.

(b) Corresponding to different incident and observation angle, on some special frequency points, there are many singularities named resonant frequencies of the antenna.

The resonant frequency is an important quantity when we consider the scattering of the slot antenna. To further searching the factors and the position of the resonant frequency, we calculate the scattering of two slots on a waveguide. Fig. 5 shows the RCS of the two slots on a waveguide with different number basis function. The incident angle is $\vartheta_i = 45^\circ$, $\varphi_i = 0^\circ$, the observation angle is $\vartheta_s = 45^\circ$, $\varphi_s = 0^\circ$. Fig. 6 shows the RCS of the same structure as $N = 5$ and at different incident angles.

From Figs. 4–5, we may conclude that the number of basis functions must be selected properly in order to increase the accuracy. Moreover, from Fig. 6, one can conclude that the points of resonant frequency not

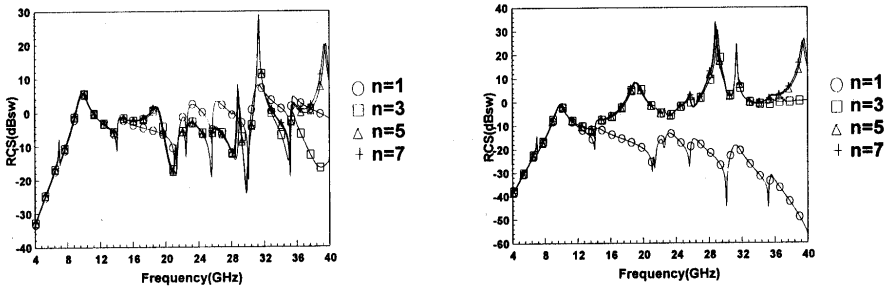

(a) $\vartheta_i = 15°, \varphi_i = 0°, \vartheta_s = 15°, \varphi_s = 0°$

(b) $\vartheta_i = 45°, \varphi_i = 0°, \vartheta_s = 45°, \varphi_s = 0°$

Figure 4. RCS of a slot in a waveguide terminated with a perfect conductor.

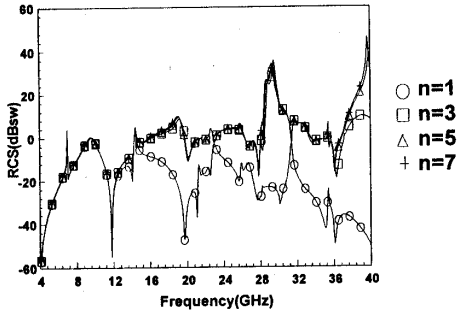

Figure 5. RCS of two slots in a waveguide terminated with a perfect conductor with different basis function.

only depends on the incident and observation angle, but also depends on the number of slots. The smaller the angle between the incident direction and the unit normal to surface of the antenna, the nearer the positions of resonant frequencies are where the length of slot is equal to the integral multiple of half wave length.

On the other hand, by theory and calculation, it is found that the points of resonant frequencies are also dependent on the length of slots. The distance of slots, the number of slots and their coupling. When the scattering of the slot antennas is calculated, the characteristics of frequency should be thought over.

In order to illuminate it more exactly on the center frequency of the bands of C, X, Ku, and Ka, we calculate the RCS of the slot antenna on the waveguide with 544 slots. The configuration of the structure is

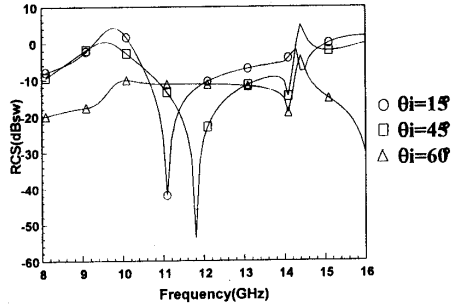

Figure 6. RCS of two slots in a waveguide terminated with a perfect conductor with different incident angle.

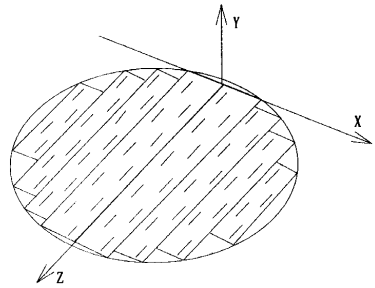

Figure 7. Geometry of wave-guide slots antenna.

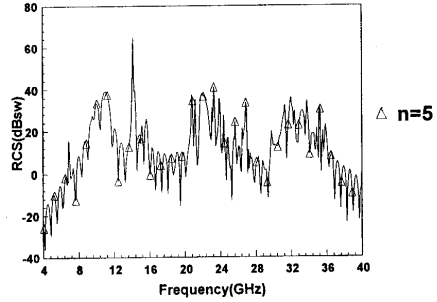

Figure 8. RCS of the slot antenna on waveguide with 544 slots.

given in Fig. 7. The RCS of this structure is displayed in Fig. 8, where $n = 5,\ \vartheta_i = 45°,\ \varphi_i = 0°,\ \vartheta_s = 45°,$ and $\varphi_s = 0°$. Note that at these center frequencies and the given incident angle the bistatic RCS of the antenna may be calculated exactly.

4. CONCLUSION

In this paper, a numerical technique for analyzing on the scattering of the slot antennas fed by waveguides is presented. In this technique, the MOM/EECs are employed. Numerical results in the form of the RCS of the slot antenna over a large frequency are presented and the resonant frequency is analyzed. By calculating, it is shown that the method is faster and applicable, especially on back/bistatic RCS of the slot antennas. These problems will be discussed in the following paper.

REFERENCES

1. Chen, J., and J. Jin, "Electromagnetic scattering from slot antennas on waveguides with arbitrary terminations," *Microwave and Optical Technology Letters,* Vol. 10, No. 5, 286–291, 1995.
2. Josefsson, L. G., "Analysis of longitudinal slots in rectangular waveguides," *IEEE Trans. Antenna and Propagation,* Vol. 35, No. 12, 1351–1357, 1987.
3. Fan, G. X., and J. M. Jin, "Scattering from a cylindrically conformal slotted waveguide array antenna," *IEEE Trans. Antennas and propagation,* Vol. 45, No. 7, 1150–1159, 1997.
4. Josefsson, L., "Slot coupling and scattering," in *IEEE Antennas Propagation Int. Symp.,* Dallas, TX, 942–945, June 1990.
5. Murrasaki, T., and M. Ando, "Equivalent edge currents by the modified edge representation: physical optics components," *IEIEC Trans. on Electron,* E75-C, No. 5, 617–626, 1991.
6. Wu, Z., and M. Zhang, "Improved equivalent edge currents by modified edge representation and their application in EM scattering," *Acta Electronica Sinica,* No. 9, 1998.